

Lightning, the Science. Part 2: Current and Electromagnetics

RAKOV V.A.

Florida University, Gainesville, Fl, USA

Lightning can be defined as a transient, high-current (typically tens of kA) electric discharge in air whose length is measured in km. As for any discharge in air, lightning channel is composed of ionized gas, that is, of plasma, whose peak temperature is typically 30,000 K, about five times higher than the temperature of the surface of the Sun. The global lightning flash rate is some tens to a hundred km per second. Lightning initiates many forest fires, and over 30% of all electric power line failures are lightning related. Each commercial aircraft is struck by lightning on average once a year. A lightning strike to an unprotected object or system can be catastrophic. In the first part [1] of the article, an overview of thunderclouds and their charge structure was given, and different types of lightning were described. The existing hypotheses of lightning initiation in thunderclouds were reviewed. In the second part of the article, current and electromagnetic signatures of lightning are characterized and the techniques to measure lightning electric and magnetic fields are discussed.

Key words: lightning, first and subsequent strokes, lightning peak current, measurements of lightning electric and magnetic fields

Current and Electromagnetic Field Signatures.

The most complete characterization of the return stroke in negative downward flashes is due to Karl Berger and co-workers (e.g., [2, 3]). The data of Berger were derived from oscillograms of current measured using resistive shunts installed at the tops of two 70-m high towers on the summit of Monte San Salvatore in Lugano, Switzerland. The summit of the mountain is 915 m above sea level and 640 m above the level of Lake Lugano, located at the base of the mountain. The towers are of moderate height, but because the mountain contributed to the electric field enhancement near the tower tops, the effective height of each tower was a few hundred meters. As a result, the majority of lightning strikes to the towers were of the upward type. Here we only consider return strokes in negative downward flashes. A total of 101 are included in the summary by Berger et al. [3]. Berger's data were additionally analyzed by Anderson and Eriksson [4].

The results of Berger et al. [3] are still used to a large extent as the primary reference source for both lightning protection and lightning research. These results are presented in Fig. 1 and 2 and in Table.

Fig. 1 shows, on two-time scales, *A* and *B*, the average current waveshapes for negative first and subsequent strokes. The averaging procedure involved the normalization of waveforms from many strokes to their respective peak currents (so that all have peaks equal to unity) and subsequent alignment using the 0.5 peak point on the initial rising portion of the waveforms. The overall duration of the current waveforms is some hundreds of microseconds. The rising portion of the first-stroke waveform has a characteristic concave shape. The averaging procedure masked secondary maxima typically observed in first-stroke waveforms and generally attributed to major branches.

Fig. 2 shows the cumulative statistical distributions (solid-line curves) of return-stroke peak currents for (1) negative first strokes, (2) negative subsequent strokes, and (3) positive strokes (each was the only stroke in a flash). These empirical distributions are approximated

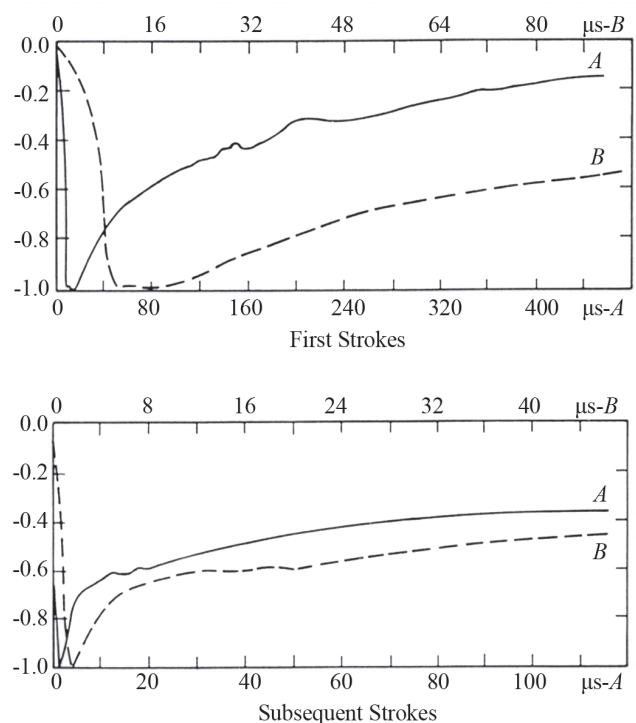


Fig. 1. Average negative first- and subsequent-stroke waveshapes each shown on two-time scales, *A* and *B*. The lower time scales (*A*) correspond to solid curves, while the upper time scales (*B*) correspond to broken curves. The vertical (amplitude) scale is in relative units, the peak values being equal to negative unity. Adapted from Berger et al. [3]

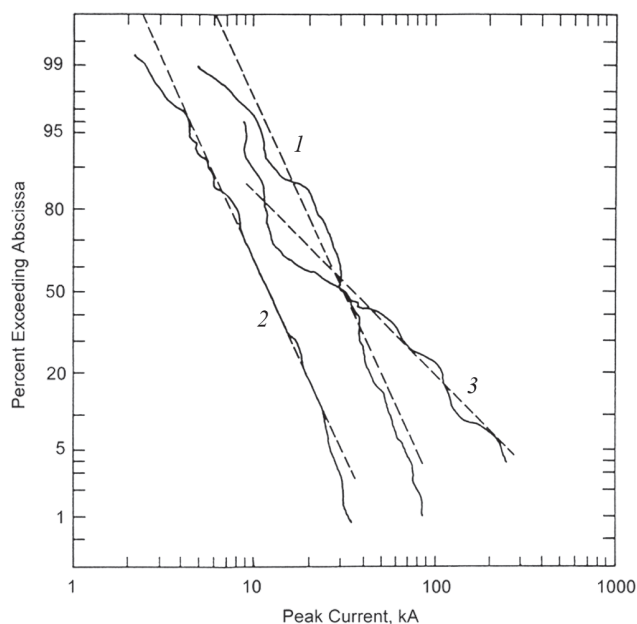


Fig. 2. Cumulative statistical distributions of return stroke peak current (solid curves) and their log normal approximations (broken lines) for (1) negative first strokes, (2) negative subsequent strokes, and (3) positive first (and only) strokes, as reported by Berger et al. [3]

by log-normal distributions (dashed lines) and shown on cumulative probability distribution graph paper, on which a Gaussian (normal) cumulative distribution appears as a slanted straight line, with the horizontal (peak current) scale being logarithmic (base 10). The vertical scale gives the percentage of peak currents exceeding a given value on the horizontal axis. The vertical scale is symmetrical with respect to the 50% value and does not include the 0 and 100% values; it only asymptotically approaches those. For a lognormal distribution, the 50% (median) value is equal to the geometric mean value.

The lightning peak current distributions for negative first and subsequent strokes (Fig. 2) are also characterized by their 95%, 50%, and 5% values based on the log normal approximations in Table, which contains a number of other parameters derived from the current oscillograms. The minimum peak current value included in the distributions is 2 kA, although no first strokes (of either polarity) with peak currents below 5 kA were observed.

Berger’s peak current distributions for first and subsequent negative strokes are generally confirmed by more recent direct current measurements, particularly those with larger sample sizes obtained in Japan (first strokes, $N = 120$; Takami and Okabe [5]), Austria (subsequent strokes, $N = 615$; Diendorfer et al., [6]), and Florida

Table

**Parameters of downward negative lightning derived from channel-base current measurements.
Adapted from Berger et al. [3]**

Parameters	Units	Sample Size	Percent Exceeding Tabulated Value		
			95%	50%	5%
Peak current (minimum 2 kA)					
First strokes	kA	101	14	30	80
Subsequent strokes		135	4.6	12	30
Charge (total charge)					
First strokes	C	93	1.1	5.2	24
Subsequent strokes		122	0.2	1.4	11
Complete flash		94	1.3	7.5	40
Impulse charge (excluding continuing current)					
First strokes	C	90	1.1	4.5	20
Subsequent strokes		117	0.22	0.95	4
Front duration (2 kA to peak)					
First strokes	μs	89	1.8	5.5	18
Subsequent strokes		118	0.22	1.1	4.5
Maximum dI/dt					
First strokes	$\text{kA } \mu\text{s}^{-1}$	92	5.5	12	32
Subsequent strokes		122	12	40	120
Stroke duration (2 kA to half peak value on the tail)					
First strokes	μs	90	30	75	200
Subsequent strokes		115	6.5	32	140
Action integral ($\int I^2 dt$)					
First strokes	A^2s	91	6.0×10^3	5.5×10^4	5.5×10^5
Subsequent strokes		88	5.5×10^2	6.0×10^3	5.2×10^4
Time interval between strokes	Ms	133	7	33	150
Flash duration					
All flashes	ms	94	0.15	13	1100
Excluding single-stroke flashes		39	31	180	900

(subsequent strokes, $N = 165$; Schoene et al. [7]). At the same time, direct current measurements in Brazil (Visacro et al. [8]) yielded 50% higher median peak currents for both first ($N = 38$) and subsequent ($N = 71$) strokes.

It follows from Fig. 2 and Table that the median return-stroke current peak for first strokes is 2 to 3 times higher than that for subsequent strokes. Also, negative first strokes transfer about a factor of four larger charge than do negative subsequent strokes. On the other hand, subsequent return strokes are characterized by 3 to 4 times higher current maximum steepness (current maximum rate of rise or maximum dI/dt).

It is important to note that the maximum dI/dt reported by Berger et al. [3] and given in Table is an underestimate of the actual value due to the limited time resolution of oscillographic data. (The mean value of maximum dI/dt reported for rocket-triggered-lightning strokes (see [1]) by Leteinturier et al. [9] is 110 kA/ μ s.) As seen in Fig. 2, only a few percent of negative first strokes are expected to exceed 100 kA, while about 20% of positive strokes have been observed to do so. On the other hand, the 50% (median) values of the current distributions for negative first and positive strokes are similar. The action integral (also referred to as specific energy) in Table represents the energy that would be dissipated in a 1- Ω resistor if the lightning current were to flow through it. It is thought that the heating of electrically conducting materials and the explosion of nonconducting materials is, to a first approximation, determined by the value of the action integral. Note that the interstroke interval in Table is likely mislabeled by Berger et al. [3] and is actually the no-current interval, that is, the interstroke interval excluding any continuing current.

Next, we will discuss typical electric and magnetic field waveforms produced by both first and subsequent return strokes at ground level at distances ranging from 1 to 200 km. These waveforms, which are drawings based on many measurements acquired in Florida by Lin et al. [10], are reproduced in Fig. 3.

The electric fields of strokes observed within a few kilometers of the flash, shown in Fig. 3, are, after the first few tens of microseconds, dominated by the electrostatic component of the total electric field, the only field component which is nonzero after the stroke current has ceased to flow. The close magnetic fields at similar times are dominated by the magnetostatic component of the total magnetic field, the component that produces the magnetic field humps seen in Fig. 3. Distant electric and magnetic fields have essentially identical waveshapes and are usually bipolar, as illustrated in Fig. 3. The data of Lin et al. [10] suggest that at a distance of 50 km and beyond, both electric and magnetic field waveshapes are dominated by their respective radiation components.

The initial field peak evident (Fig. 3) is the dominant feature of the electric and magnetic field waveforms beyond about 10 km. This initial peak also is a significant

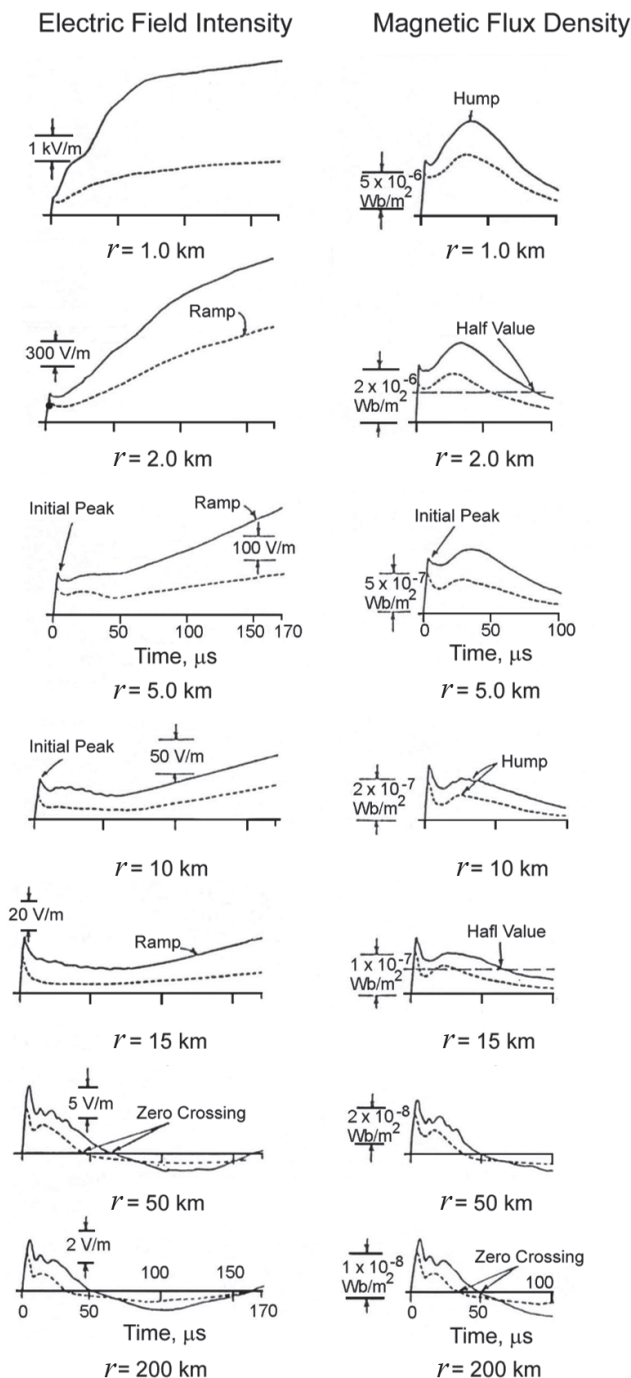


Fig. 3. Typical vertical electric field intensity (left column) and azimuthal magnetic flux density (right column) waveforms for first (solid line) and subsequent (broken line) return strokes at distances of 1, 2, 5, 10, 15, 50, and 200 km. Adapted from Lin et al. [10]

feature of waveforms from strokes between a few and about 10 km and can be identified, with some effort, in waveforms for strokes as close as a kilometer. The initial field peak is due to the radiation component of the total field and, hence, decreases inversely with distance in the absence of significant propagation effects. The field peaks produced by different return strokes at known distances can be range normalized for comparison, for example, to

100 km by multiplying the measured field peaks by $r/10^5$, where r is the stroke distance in meters. The geometric mean of the electric field initial peak value, normalized to 100 km, is typically about 6 V/m for first strokes and 3 V/m for subsequent strokes. Since the initial electric field peak appears to obey a log-normal distribution, the geometric mean value (equal to the median value for a log-normal distribution) is probably a better characteristic of the statistical distribution of this parameter than the mean (arithmetic mean) value. Note that the geometric mean value for a log-normal distribution is lower than the corresponding mean value and higher than the modal (most probable) value.

Lightning peak currents can be estimated from measured electric or magnetic fields, for which a field-to-current conversion procedure (a model-based or empirical formula) is required. The vertical component of electric field and the azimuthal component of magnetic field are usually employed.

Rakov et al. [11] proposed the following empirical formula (linear regression equation) to estimate the negative return-stroke peak current, I , from the initial electric field peak, E , and distance, r , to the lightning channel:

$$I = 1.5 - 0.037Er, \tag{1}$$

where I is in kA and taken as negative, E is positive and in V/m, and r is in km.

Eq. (1) was derived using data for 28 triggered-lightning strokes acquired by Willett et al. [12] at the Kennedy Space Center (KSC), Florida. The fields were measured at about 5 km and their initial peaks were assumed to be pure radiation. The currents were directly measured at the lightning channel base.

Lightning peak currents can also be estimated using the radiation-field-to-current conversion equation based on the transmission line (TL) model (Uman and McLain [13]), which for the electric field is given by:

$$I = \frac{2\pi\epsilon_0 c^2 r}{v} E, \tag{2}$$

where ϵ_0 is the permittivity of free space; c is the speed of light; v is the return-stroke speed (assumed to be constant).

The return-stroke speed is generally unknown and its range of variation is from one-third to two-thirds of the

speed of light. Both I and E in Eq. (2) are absolute values. The equation is thought to be valid for instantaneous values of E and I at early times (for the initial rising portion of the waveforms, including the peak).

Lightning Measurements. Measurements of lightning electric and magnetic fields are considered. Both the principles and practical aspects are covered.

A sensor that is commonly used to measure the lightning vertical electric field is a metallic disk placed flush with the ground surface, the so-called flat-plate antenna. Fig. 4,a schematically shows such an antenna, where it is assumed that the area A of the antenna sensing plate is small enough to consider the electric field E constant over that area and C_a is the capacitance of the antenna. The downward directed electric field induces negative charge Q on the surface of the antenna, which can be found as the product of the surface charge density ρ_s and the area A of the antenna sensing plate. From the boundary condition on the vertical component of electric field on the surface of good conductor

$$\rho_s = \epsilon_0 E,$$

where ϵ_0 is the electric permittivity of free space, and hence $Q = \epsilon_0 EA$.

If E is varying with time, there will be current $I = dQ/dt = \epsilon_0 A dE/dt$ flowing via C_a to ground. This current is proportional to dE/dt . In order to measure E , it is necessary to use an integrating capacitor $C \gg C_a$, (see Fig. 4,b), since C_a is usually too small for measuring lightning fields.

Thus, the voltage across the integrating capacitor (capacitive voltage drop) will be

$$V_{out} = \frac{1}{C_a + C} \int_0^t I(t') dt' \approx \frac{1}{C} \int_0^t I(t') dt' = \frac{Q}{C} = \frac{\epsilon_0 AE}{C}. \tag{3}$$

Strictly speaking, Eq. (3) applies only to the case of infinitely large input impedance of the recorder. In practice, the input resistance of the recorder (or fiber-optic-link transmitter) plays an important role, limiting the time interval or the lower end of the frequency range over which Eq. (3) is valid.

To examine this further, it is convenient to use the Norton equivalent circuit of the antenna, which is the antenna short-circuit current, $I = \epsilon_0 A j\omega E$ (ideal current

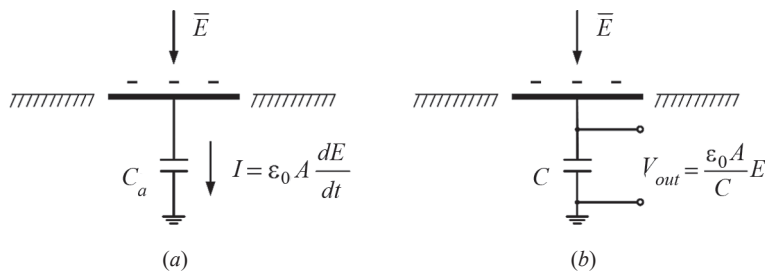


Fig. 4. Illustration of the principle of operation of the flat-plate antenna:

a – Antenna without external circuit; b – Antenna with external integrating capacitor $C \gg C_a$. Drawing by Potao Sun

source), in parallel with antenna impedance, $1/j\omega C_a$, where $\omega = 2\pi f$ with f being frequency in hertz. The equivalent circuit including the Norton equivalent of the antenna, integrating capacitance, and input resistance R_{in} and capacitance C_{in} of the recorder is shown in Fig. 5.

Since $C \gg C_a$ and usually $C \gg C_{in}$, the current basically splits between C and R_{in} , and Eq. (3) holds when $1/\omega C \ll R_{in}$; that is, $\omega \gg 1/(R_{in}C)$ or $f \gg 1/(2\pi R_{in}C)$.

In the time domain, Eq. (3) is valid when the variation time (duration) of the signal of interest $\Delta t \ll \tau$, where $\tau = R_{in}C$ is the decay time constant of the measuring system (when E is a step-function, V_{out} will exponentially decay to $1/e$, where e is the base of the natural logarithm, or about 37% of its initial value over the time equal to τ).

For example, if $C = 1 \mu F$ and $R_{in} = 1 M\Omega$, $\tau = 1$ s, long enough for recording electric fields produced by lightning processes occurring on time scales of the order of tens of milliseconds (for example, stepped leaders or return strokes followed by continuing currents). Typical values of C_a and C_{in} are of the order of tens to hundreds of picofarad ($1 \text{ pF} = 10^{-12} \text{ F}$) or less, clearly much smaller than $C = 1 \mu F$ (10^{-6} F) in this example. For recording return-stroke pulses, τ of the order of milliseconds is usually sufficient, while for the faithful reproduction of overall flash waveforms it should be of the order of 10 s or so.

For recording microsecond- and submicrosecond-scale pulses, τ shorter than a millisecond or so can be used. Measuring systems with decay time constants of the order of seconds are sometimes referred to as “slow antenna” systems, and those with submillisecond time constants as “fast antenna” systems. “Fast-antenna” systems usually have higher gains than “slow-antenna” ones. The terms “slow” and “fast” have nothing to do with the upper frequency response of the system, which is usually determined by the amplifier or fiber-optic link. The measuring system shown in Fig. 5 employs a passive integrator. In the case of active integrator, $\tau = RC$ is determined by R and C connected in parallel in the feedback circuit of the operational amplifier.

We now discuss the situation when the condition of $\Delta t \ll \tau$ is not satisfied. Such situations are not rare. Indeed, since the range of lightning electric field changes is very large (it spans orders of magnitude), it is practically impossible to build a single measuring system that would have a dynamic range suitable for recording all those changes. Smaller field changes require a higher gain that usually leads to system saturation by larger field changes.

On the other hand, a lower gain needed to keep the larger field changes on scale would render the smaller field changes unresolved. The larger field changes are usually relatively slow, varying on time scales of the order of milliseconds and longer (e.g., electric field changes produced by long continuing currents), while the smaller field changes are usually microsecond-scale pulses. One way to enable a field measuring system to record relatively small and relatively short pulses is to allow the larger and slower field changes to decay with a relatively short time

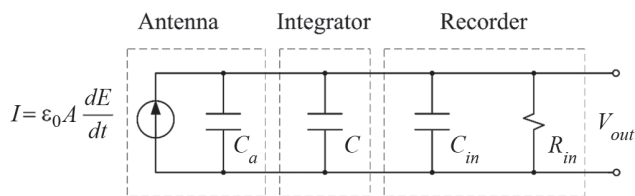


Fig. 5. Norton equivalent circuit of electric field antenna shown along with the integrating capacitance and the input impedance of recorder (usually $C \gg C_a$ and $C \gg C_{in}$). Drawing by Potao Sun

constant. In order to avoid distortion of the pulses, this time constant should be much longer than the expected duration of the pulses. As discussed above, time constants satisfying the latter requirement are shorter than a millisecond or so. In this case, some associated field changes varying on a millisecond time scale (e.g., overall field changes produced by K- and M-processes) will be distorted. Specifically, ramp-like electric field changes due to lightning K-processes can be converted to pulses, with the falling edge of the pulse being due to instrumental decay, as opposed to occurring in response to source variation. In principle, the instrumental decay can be compensated in postprocessing of measured field waveforms, to remove the distortion and reconstruct the undistorted waveform (Rubinstein et al. [14]).

Placement of flat-plate antenna flush with the ground ensures that the electric field to be measured is not influenced by the antenna. This gives an advantage of theoretical calibration of the measuring system (see Eq. (3)). Any antenna elevated above the ground surface will enhance the field that would exist at the same location in the absence of antenna.

As a result, experimental calibration is required to determine the field enhancement factor (except for the spherical antenna with isolated cutouts, for which the enhancement factor is known; it is equal to 3) the inverse of which is to be used as a multiplier in Eq. (3). Calibration can be done by placing the antenna in a uniform field of a large parallel-plate capacitor or by comparing the antenna output with that of a flush-mounted reference antenna. When calibration is done experimentally, an antenna of any geometry (e.g., a vertical rod (monopole) with or without capacitive loading at its top or an inverted antenna with a grounded “bowl” above the elevated sensing plate) can be used. However, slender antennas are generally not used for measuring fields at short distances from the lightning channel. Such antennas can enhance the electric field to a degree that corona discharge occurs from the antenna. It is impossible to accurately measure electric fields in the presence of corona from the antenna, since, besides the current charging the antenna, there will be corona current transporting charges into the air surrounding the antenna, both currents flowing through the same integrating capacitor across which the output voltage is measured.

If an essentially flush with the surface flat-plate antenna is installed on the roof of a building or other structure, another field enhancement factor, due to the presence

of the building, is to be taken into account. This latter enhancement factor can be calculated numerically. For example, Baba and Rakov [15], who used the 3-D finite-difference time-domain (FDTD) method, estimated that for a building having a plan area of 40×40 m² and a height of 20 m the electric field enhancement factor (at the center point of its flat roof) is 1.5 and it is 3.0 if the height of the building is 100 m. For comparison, the enhancement factor on the top of hemispherical structure is independent of its size and equal to 3. The magnitude of vertical electric field at ground level in the immediate vicinity of the building is reduced relative to the case of no building, with this shielding effect becoming negligible at horizontal distances from the building exceeding twice the height of the building. In contrast to the electric field, the magnitude of magnetic field was found to be not much influenced by the presence of building. Note that Baba and Rakov (Table VI) [15] showed that the electric field enhancement due to the presence of building is only slightly influenced by building conductivity ranging from 1 mS/m (dry concrete) to infinity and essentially independent of relative electric permittivity ranging from 1 to 10.

The use of long horizontal coaxial cables between the antenna and the associated electronics should be avoided, since the horizontal component of electric field (present due to the finite ground conductivity) can induce unwanted voltages in these cables. The horizontal electric field waveshape is similar to that of the derivative of the vertical field. As a result, the measured field waveform may be a superposition of the vertical field, which is being measured, and the unwanted horizontal field, which causes a distortion of the vertical field waveform by making peaks and valleys sharper than they actually are in the vertical field (Uman [16]). The problem can be solved by using a fiber-optic link instead of the coaxial cable. Further, significant reduction of noise can be achieved by digitizing signals at the antenna location and digitally transmitting them to recorder.

One can check if the electric field measuring system is working properly by comparing electric field waveforms produced by individual lightning events (e.g., return strokes) with the corresponding magnetic field waveforms. At large distances (> 50 km or so), those waveforms are dominated by their radiation components and, hence, their shapes should be identical. Further, the ratios of electric and magnetic field peaks at large distances for sources near ground (return strokes) should be equal to the speed of light ($E/B = c$).

If in Fig. 4, *b* and 5 the integrating capacitor C is replaced with the resistor R (such that $R \ll 1/(\omega C_a)$ and $R \ll 1/(\omega C_{in})$), the output voltage is proportional to dE/dt . Measured dE/dt waveforms can be numerically integrated over time to obtain E waveforms, although the integration interval should not be too long in order to avoid accumulation of significant error.

To measure the magnetic field produced by lightning processes a loop of wire can be used as an antenna. According to Faraday's Law, a time varying magnetic field passing through an open-circuited loop of wire will induce a voltage (electromotive force) at the terminals of the loop (see Fig. 6).

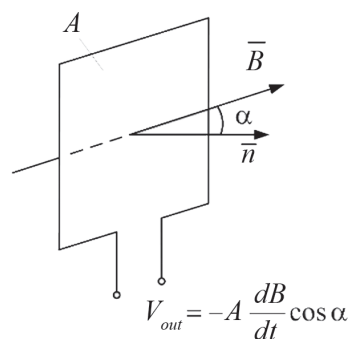


Fig. 6. Illustration of the principle of operation of the loop antenna. Drawing by Potao Sun

The induced voltage is proportional to the rate of change of magnetic flux passing through the loop area. Assuming that the loop area, A , is small enough to consider the normal component of magnetic flux density, $B_n = B \cos \alpha$, where α is the angle between the magnetic flux density vector and the normal to the plane of the loop, to be constant over that area, we can express the magnitude of induced voltage as follows:

$$V = A \frac{dB_n}{dt}. \quad (4)$$

When $\cos \alpha = 1$ ($\alpha = 0$), the induced voltage is maximum, and when $\cos \alpha = 0$ ($\alpha = 90^\circ$), the induced voltage is zero. It follows, that a vertical loop antenna in a fixed position is directional in that the magnitude of voltage induced across its terminals is a function of the direction to the source, and two such antennas with orthogonal planes can be used for magnetic direction finding. In order to obtain the horizontal (azimuthal) component of magnetic field, which is the dominant component for essentially vertical lightning channels, two vertical loop antennas are required, unless the direction to the lightning channel is known (for example, in the case of rocket-triggered lightning; see [1]).

Since the signal at the output of a loop antenna is proportional to the magnetic field derivative, the signal must be integrated to obtain the field. This can be accomplished using either an RC or RL circuit, or the measured field derivative signal can be integrated numerically. We will consider below the case of RC integrator. In the following, we will assume that B is normal to the plane of the loop antenna ($\alpha = 0$), so that $B = B_n$. The voltage induced at the terminals of a loop antenna is the open-circuit voltage, $A dB/dt$ or $A j\omega B$, and, hence, it can be used for building the Thevenin equivalent circuit of the antenna. The source impedance is predominantly inductive, $j\omega L$. The overall equivalent circuit including, besides the antenna, the RC integrator and input impedance (input resistance in parallel with input capacitance) of the recorder is shown in Fig. 7.

In contrast with the electric field antenna (see Fig. 5), the integrating capacitor in Fig. 7 has two discharge paths, one through the input resistance of the recorder (similar to Fig. 5) and the other through resistor R of the integrating

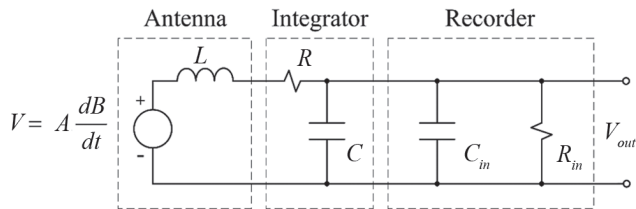


Fig. 7. Thevenin equivalent circuit of magnetic field antenna shown along with the integrating circuit and the input impedance of recorder. Drawing by Potao Sun

circuit and the source (the ideal voltage source has zero impedance). As a result, there are three conditions for undistorted recording of magnetic field with the measuring system shown in Fig. 7. The first one, $R \gg 1/\omega C$ ($\omega \gg 1/(RC)$; C_{in} is neglected), determines the lower frequency limit and is equivalent to the $\Delta t \ll \tau$ ($\tau = RC$) condition. The second one, $R \gg \omega L$ ($\omega \ll R/L$), determines the upper frequency limit. The third one, $R_{in} \gg R$, requires that C discharges through R , not R_{in} . Under those three conditions, the output voltage is independent of frequency and given by

$$V_{out} = \frac{AB}{RC}. \quad (5)$$

Magnetic field measuring circuits are rarely passive; active integrators and amplifiers are usually required. A loop antenna developed by George Schnetzer and used by the University of Florida Lightning Research Group is described in Section 7.2 of Rakov [17].

In designing field measuring systems, one needs to know expected magnitudes and durations of signals to be recorded. Different lightning processes produce different electromagnetic signatures, these signatures change with distance, and at the same distance there is large variation in source strength. Both variations in the source and with distance should be considered. Given below is a brief review of characteristics of lightning electric and magnetic fields expected at different distances from the source.

At ground level and at distances greater than a few kilometers, the initial electric field peak is dominated by its radiation component. Typical electric field peak values normalized to 100 km are about 6 V/m and 3 V/m for negative first and subsequent return strokes, respectively. The largest radiation field peaks due to stepped and dart-stepped leaders are typically a factor of 10 smaller than the corresponding return-stroke field peak at the same distance. Radiation fields vary inversely with distance ($1/r$ dependence), if propagation effects due to finite ground conductivity can be neglected. Generally, the typical radiation field peak values normalized to 100 km can be scaled to either smaller or larger distances in the range from about 5 to about 200 km. For example, if the field peak at 100 km is 6 V/m, it is expected to be 60 V/m at 10 km and 3 V/m at 200 km. The corresponding magnetic radiation field peaks can be readily found by dividing the electric field peak by the speed of light (3×10^8 m/s) to find the magnetic flux density (B) and by the intrinsic

impedance of free space (377Ω) to find the magnetic field intensity (H). At a given distance, the field can be at least a factor of 5 greater and a factor of 5 smaller, due to variation in the source.

Summary. An understanding of the physical properties and deleterious effects of lightning is critical to the adequate protection of power and communication lines, aircraft, spacecraft, and other objects and systems. In the first part [1] of the article, the characteristic of Thunderclouds has been given and their Charge structure has been considered. Basic terminology has been introduced, and different types of lightning have been described. For the most common negative cloud-to-ground lightning, main lightning processes have been identified and the existing hypotheses of lightning initiation in thunderclouds have been reviewed. In the second part of the article, the current and electromagnetic field signatures have been considered. Typical electric and magnetic field waveforms produced by both first and subsequent return strokes at ground level at distances ranging from 1 to 200 km have been discussed. Both the principles and practical aspects of lightning electric and magnetic fields measurements have been considered. Given is a brief review of characteristics of lightning electric and magnetic fields expected at different distances from the source.

REFERENCES

1. Rakov V.A. Lightning, the Science. Part 1: Modern View. – *Elektrichestvo*, 2021, No. 5, pp. 4–16.
2. Berger K. Methods and results of the lightning research on the Monte San Salvatore near Lugano in the years 1963–1971. – *Bull. SEV* 63, 1972, No. 24, pp. 1403–1422.
3. Berger K., Anderson R. B., Kroninger H. Parameters of lightning flashes. – *Electra*, 1975, No. 41, pp. 23–37.
4. Anderson R.B., Eriksson A.J. Lightning parameters for engineering application. – *Electra*, 1980, vol. 69, pp. 65–102.
5. Takami, J., Okabe S. Observational results of lightning current on transmission towers. – *IEEE Trans. Power Delivery*, 2007, vol. 22, pp. 547–556.
6. Diendorfer G., Pichler H., Mair M. Some parameters of negative upward-initiated lightning to the Gaisberg tower (2000–2007). – *IEEE Trans. Electromagn. Compat.*, 2009, vol. 51, pp. 443–452.
7. Schoene J., Uman M.A., Rakov V.A., et al. Characterization of return-stroke currents in rocket-triggered lightning. – *Journal of Geophysical Research*, 2009, vol. 114, pp. D03106, doi:10.1029/2008JD009873.
8. Visacro S., Mesquita C.R., De Conti A., Silveira F.H. Updated statistics of lightning currents measured at Morro do Cachimbo station. *Atmos. Res.*, 2012, vol. 117, pp. 55–63.
9. Leteinturier C., Hamelin J. H., Eybert-Berard A. Submicrosecond characteristics of lightning return-stroke currents. – *IEEE Trans. Electromagn. Compat.*, 1991, vol. 33, pp. 351–357.
10. Lin Y.T., Uman M.A., Tiller J.A., Brantley R.D., Beasley W.H., Krider E.P., Weidman C.D. Characterization of lightning return stroke electric and magnetic fields from simultaneous two station measurements. *J. Geophys. Res.*, 1979, vol. 84, pp. 6307–6314.
11. Rakov V.A., Thottappillil R., Uman M.A. On the empirical formula of Willett et al. relating lightning return-stroke peak current and peak electric field. *J. Geophys. Res.*, 1992, vol. 97, No. 11, pp. 527–533.
12. Willett J.C., Bailey J.C., Idone V.P., Eybert Berard A., Barret L. Submicrosecond intercomparison of radiation fields and currents in triggered lightning return strokes based on the transmission line model. *J. Geophys. Res.*, 1989, vol. 94, No. 13, pp. 275–286.

13. **Uman M.A., McLain D.K.** Magnetic field of the lightning return stroke. *J. Geophys. Res.* 1969, vol. 74, pp. 6899–6910.

14. **Rubinstein M., Bermúdez J.-L., Rakov V.A., Rachidi F., Hussein A.** Compensation of the instrumental decay in measured lightning electric field waveforms. – *IEEE Trans. on EMC*, 2012, vol. 54, No. 3, pp. 685–688.

15. **Baba Y., Rakov V.A.** 2007. Electromagnetic fields at the top of a tall building associated with nearby lightning return strokes. – *IEEE Trans. Electromagn. Compat.*, vol. 49, No. 3, pp. 632–643.

16. **Uman M.A.** *The Lightning Discharge*. Orlando (Fla): Academic Press, 1987, 391 p.

17. **Rakov V.A.** *Fundamentals of Lightning*, Cambridge University Press, 2016, 257 p.

[25.12.2020]



The author: **Rakov Vladimir A.** (Florida University, Gainesville, Florida, USA) – Professor of Dept. for Electrical and Computer Engineering, PhD.

Электричество, 2021, № 6, с. 4–11

DOI:10.24160/0013-5380-2021-6-4-11

Молния, Наука. Часть 2: Ток и электромагнетизм

РАКОВ Владимир А. – PhD, профессор, Университет во Флориде (г. Гейнсвилл, Флорида, США)

Молния может быть определена как переходный, многоамперный (обычно десятки кА) электрический разряд в воздухе, длина которого измеряется в км. Как и любой разряд в воздухе, канал молнии состоит из ионизированного газа, то есть плазмы, пиковая температура которой обычно составляет 30000 К, что примерно в пять раз выше температуры поверхности Солнца. Глобальная скорость вспышки молнии составляет от нескольких десятков до ста км/с. Молния инициирует многие лесные пожары, и более 30% всех отказов линий электропередачи связаны с молнией. Каждый коммерческий самолет поражается молнией в среднем раз в год. Удар молнии в незащищенный объект или систему может быть катастрофическим. В первой части статьи [1] был дан обзор грозовых облаков и их зарядовой структуры, а также описаны различные типы молний. Рассмотрены существующие гипотезы возникновения молний в грозовых облаках. Во второй части дается характеристика токовых и электромагнитных сигнатур молнии и рассматриваются методы измерения электрических и магнитных полей, генерируемых вспышками молнии.

Ключевые слова: молния, первый и последующие удары, пиковый ток молнии, измерения электрических и магнитных полей молнии

СПИСОК ЛИТЕРАТУРЫ

1. **Рakov V.A.** *Lightning, the Science. Part 1: Modern View.* – *Электричество*, 2021, № 5, с.4–16.

2. **Berger K.** Methods and results of the lightning research on the Monte San Salvatore near Lugano in the years 1963-1971. – *Bull. SEV* 63, 1972, No. 24, pp. 1403–1422.

3. **Berger K., Anderson R.B., Kroninger H.** Parameters of lightning flashes. – *Electra*, 1975, No. 41, pp. 23–37.

4. **Anderson R.B., Eriksson A.J.** Lightning parameters for engineering application. – *Electra*, 1980, vol. 69, pp. 65–102.

5. **Takami, J., Okabe S.** Observational results of lightning current on transmission towers. – *IEEE Trans. Power Delivery*, 2007, vol. 22, pp. 547–556.

6. **Diendorfer G., Pichler H., Mair M.** Some parameters of negative upward-initiated lightning to the Gaisberg tower (2000–2007). – *IEEE Trans. Electromagn. Compat.*, 2009, vol. 51, pp. 443–452.

7. **Schoene J., Uman M.A., Rakov V.A., et al.** Characterization of return-stroke currents in rocket-triggered lightning. – *Journal of Geophysical Research*, 2009, vol.114, pp. D03106, doi:10.1029/2008JD009873.

8. **Visacro S., Mesquita C.R., De Conti A., Silveira F.H.** Updated statistics of lightning currents measured at Morro do Cachimbo station. *Atmos. Res.* 2012, vol. 117, pp. 55–63.

9. **Leteinturier C., Hamelin J. H., Eybert-Berard A.** Submicrosecond characteristics of lightning return-stroke currents. – *IEEE Trans. Electromagn. Compat.*, 1991, vol. 33, pp. 351–357.

10. **Lin Y.T., Uman M.A., Tiller J.A., Brantley R.D., Beasley W.H., Krider E.P., Weidman C.D.** Characterization of lightning return stroke electric and magnetic fields from simultaneous two station measurements. *J. Geophys. Res.*, 1979, vol. 84, pp. 6307–6314.

11. **Rakov V.A., Thottappillil R., Uman M.A.** On the empirical formula of Willett et al. relating lightning return-stroke peak current and peak electric field. *J. Geophys. Res.*, 1992, vol. 97, No. 11, pp. 527–533.

12. **Willett J.C., Bailey J.C., Idone V.P., Eybert Berard A., Barret L.** Submicrosecond intercomparison of radiation fields and currents in triggered lightning return strokes based on the transmission line model. *J. Geophys. Res.*, 1989, vol. 94, No. 13, pp. 275–286.

13. **Uman M.A., McLain D.K.** Magnetic field of the lightning return stroke. *J. Geophys. Res.* 1969, vol. 74, pp. 6899–6910.

14. **Rubinstein M., Bermúdez J.-L., Rakov V.A., Rachidi F., Hussein A.** Compensation of the instrumental decay in measured lightning electric field waveforms. – *IEEE Trans. on EMC*, 2012, vol. 54, No. 3, pp. 685–688.

15. **Baba Y., Rakov V.A.** 2007. Electromagnetic fields at the top of a tall building associated with nearby lightning return strokes. – *IEEE Trans. Electromagn. Compat.*, vol. 49, No. 3, pp. 632–643.

16. **Uman M.A.** *The Lightning Discharge*. Orlando (Fla): Academic Press, 1987, 391 p.

17. **Rakov V.A.** *Fundamentals of Lightning*, Cambridge University Press, 2016, 257 p.

[25.12.2020]